



Development and testing of an online method to measure ambient fine particulate reactive oxygen species (ROS) based on the 2',7'-dichlorofluorescein (DCFH) assay

L. E. King and R. J. Weber

School of Earth and Atmospheric Sciences, Georgia Institute of Technology, Atlanta, GA, USA

Correspondence to: R. J. Weber (rweber@eas.gatech.edu)

Received: 17 February 2013 – Published in Atmos. Meas. Tech. Discuss.: 4 April 2013

Revised: 7 June 2013 – Accepted: 11 June 2013 – Published: 11 July 2013

Abstract. An online, semi-continuous instrument to measure fine particle ($PM_{2.5}$) reactive oxygen species (ROS) was developed based on the fluorescent probe 2',7'-dichlorofluorescein (DCFH). Parameters that influence probe response were first characterized to develop an optimal method for use in a field instrument. The online method used a mist chamber scrubber to collect total (gas plus particle) ROS components (ROS_t) alternating with gas phase ROS (ROS_g) by means of an inline filter. Particle phase ROS (ROS_p) was determined by the difference between ROS_t and ROS_g . The instrument was deployed in urban Atlanta, Georgia, USA, and at a rural site during various seasons. Concentrations from the online instrument generally agreed well with those from an intensive filter measurement of ROS_p . Concentrations of the ROS_p measurements made with this instrument were lower than reported in other studies, often below the instrument's average limit of detection ($0.15 \text{ nmol H}_2\text{O}_2 \text{ equivalents m}^{-3}$). Mean ROS_p concentrations were $0.26 \text{ nmol H}_2\text{O}_2 \text{ equivalents m}^{-3}$ at the Atlanta urban sites compared to $0.14 \text{ nmol H}_2\text{O}_2 \text{ equivalents m}^{-3}$ at the rural site.

1 Introduction

Reactive oxygen species (ROS) when introduced into a biological system have a strong tendency to disrupt the electrochemical balance. The amount of disruption depends on factors such as the amount of ROS introduced or produced within the system, the location of the introduction or production of the reactive species, the duration of the insult and

a host of other factors, many of which have yet to be ascertained in nature as well as in scope (Barrett et al., 1999; Morgan et al., 2001; Oberdörster, 2004; Rothe and Valet, 1990; Squadrito et al., 2001; Sugamura and Keaney, 2011; Xia et al., 2006). Human exposure to ROS can occur by a number of known routes. ROS associated with gaseous or particulate pollutants generated in the atmosphere may be transported into the respiratory system. Their deposition generates adverse effects within cells of that location. Compounds associated with aerosol particles may also be deposited and result in either a direct or indirect generation of ROS intracellularly, in which the oxidative stress may not be limited to the immediate area of deposition.

Reactive and oxidizing species have been shown to be detrimental to biological systems in a wide variety of ways, including disrupting protein pathways, increasing the breakdown of key cellular structures and leading to the eventual death of individual cells, prior to which large amounts of cellular stress translate into wider systemic stress in organisms (Antonini et al., 1998; Barrett et al., 1999; Squadrito et al., 2001; Sugamura and Keaney, 2011). Atmospheric exposure to ROS can occur either in the gas or particle phase. Gas phase ROS (ROS_g) is most likely to be removed in the upper mucus membranes (Kao and Wang, 2002), whereas other studies (Pope et al., 1995) have demonstrated the ability of fine particles, which would include particle phase ROS (ROS_p), to penetrate further into the lungs and deposit in the alveoli.

Atmospheric studies to measure ambient ROS have generally focused on gas phase measurements (Reeves and Penkett, 2003; Klippel et al., 2011), typically using

fluorescent probes. ROS_p measurements have primarily been made using filters for particle collection and analysis of extracts using similar probes (Hung and Wang, 2001; Venkatchari et al., 2005, 2007). These fluorescent probes, such as 2', 7'-dichlorofluorescein (DCFH) (Hung and Wang, 2001), Amplex Red (Votyakova and Reynolds, 2004), *p*-hydroxyphenylacetic acid (POHPAA) (Lee et al., 1991) and others, have been adapted from their use in intracellular ROS measurements for direct measurements in the atmosphere. Various ROS will oxidize these probes, which then fluoresce at specific wavelengths when excited. Fluorescent probes are most often chosen for their fast response rates, linear response to varying ROS concentrations and either dedicated response to a particular compound (e.g., Amplex Red) (Zhou et al., 1997) or lack of chemical specificity (e.g., DCFH; LeBel et al., 1992).

The overall findings of measurements of ambient ROS have shown some associations with other atmospheric species. ROS_p is positively correlated with both Fe concentration and other transition metals (See et al., 2007), and a positive correlation with organic concentrations (Wang et al., 2010) has been observed. Some correlations between ROS and ozone have been reported, particularly in the early to mid-afternoon (Venkatchari et al., 2005).

A potential drawback to previously reported ROS_p concentrations is that previous studies may be susceptible to sampling artifacts. Filter-based studies, particularly for reactive compounds, are likely limited by long sample collection times that may result in under-prediction of concentrations (Hung and Wang, 2001). Previous ROS_p filter studies have also been challenging due to reported high and variable blank concentrations (Hung and Wang, 2001; Venkatchari et al., 2005, 2007).

Some preliminary results exist for an online method to measure ROS_p (Venkatchari and Hopke, 2008; Wang et al., 2011). This instrument couples the particle-into-liquid sampler (PILS) with a flow system that mixes DCFH and a catalyst, peroxidase from horseradish (HRP) with the PILS sample stream-contained soluble $\text{PM}_{2.5}$ components (Venkatchari and Hopke, 2008). After utilizing mixing elements to combine and sufficiently react the sample ROS with the fluorescent reagents, the sample is measured using a spectrometer. Results from a summertime week-long field operation in Rochester, NY (Wang et al., 2011), showed an average of $8.3 \pm 2.2 \text{ nmol H}_2\text{O}_2 \text{ equivalents m}^{-3}$. This study also indicated a diurnal trend in ROS_p with an increase in daytime concentrations, as well as higher values on weekdays than on weekends. These reported values exceeded ambient values found on filters in previous studies in the USA and Taiwan (Hung and Wang, 2001; Venkatchari et al., 2005, 2007). These results appear to indicate that ROS_p loss from ambient filters can be minimized by using a continuous online system with virtually no delay between collection and analysis.

2 Materials and methods

2.1 Primary materials

For this study the DCFH probe was chosen to provide a comprehensive ROS detector. Of the ROS probes commercially available, DCFH has a long and well-documented record of sensitivity in both cellular and atmospheric aerosol applications (Hung and Wang, 2001; Liu et al., 2007; Venkatchari and Hopke, 2008; Venkatchari et al., 2005, 2007; Wang et al., 2011; Black and Brandt, 1974; Cathcart et al., 1983; LeBel et al., 1992). 2', 7'-dichlorodihydrofluorescein diacetate (DCFHDA) was purchased from both Sigma Aldrich (St. Louis, MO, USA) and Calbiochem (EMD Chemicals, Billerica, MA, USA) depending on availability. Horseradish peroxidase (HRP) (Type II) was purchased exclusively from Sigma Aldrich. Hydrogen peroxide (30%, w/w) was purchased from J.T. Baker through VWR (Atlanta, GA, USA).

Primary analytical equipment included a spectrofluorometer (Maya2000Pro, Ocean Optics, Dunedin, FL, USA) with cutoff and long-pass filters for wavelengths greater than 515 nm and a 200 μm slit. The spectrometer was further equipped with a flow-through cell of 450 μL volume with a light path of $10 \times 4 \text{ mm}$ (FIA-SMA-FL-ULT). The initial excitation source was a blue (475 nm) LED source manufactured by Mikropack (Ocean Optics, LS-475), replaced with a Jasco-manufactured 470 nm wavelength LED with adjustable voltage (LLS-470, Ocean Optics) to accommodate LED intensity loss with bulb age. Fiberoptic cables (SMA-905, Ocean Optics) completed the primary analytical apparatus.

Solutions were pumped through the flow-through cell using an 8-channel peristaltic pump (Ismatec, Opfikon, Switzerland). Any tubing, glassware or other vessels for working solution storage or transport were shielded in aluminum foil to prevent photooxidation.

2.2 Reagent preparation

According to previously published methods (Cohn et al., 2008; LeBel et al., 1992), DCFHDA was dissolved in HPLC-grade ethanol in a portable darkroom (Silver Edition HydroHut, Flora Hydroponics, Atlanta, GA, USA), and either used immediately or stored in the freezer in an amber bottle, sealed to prevent evaporation of the solvent. To prepare the working solution of a desired concentration of DCFH, 0.01 N NaOH was added to the DCFHDA solution to remove the acetate. After 30 min, the solution was buffered with a sodium phosphate buffer (pH 7.4) to halt the reaction, dilute the DCFH concentration, bringing the overall pH to 7.2 (allowable range, 7.2–7.4). pH was verified with a handheld pH monitor (VWR). A quantity of HRP (Type II, Sigma Aldrich) was then added to the solution to bring it to 0.5–1 units HRP mL^{-1} solution, based on the specific purpogallin units per milligram for each lot of HRP. The working solution

(DCFH + HRP) was then stored in an amber vessel or foil-wrapped flask in the laboratory refrigerator at 2 °C and discarded after a period of 2 days. The original standard working solution was 5 μM DCFH with 0.5 units HRP mL⁻¹ solution.

3 Offline system for calibration and sensitivity analysis of DCFH

3.1 Initial method and analysis

Initial evaluation of DCFH was conducted following the method described by Hung and Wang (2001) in which the probe was used to quantify the ROS concentrations from ambient particle filter extracts. A total of 3 mL of DCFH-HRP solution were pipetted in the darkroom into 15 mL amber centrifuge vials, which were then covered with predrilled caps (1/16" diameter) and sealed with paper laboratory tape. These preloaded vials were stored in the refrigerator until use.

For analysis, the tape was briefly removed from the vials, and 0.1 mL of either deionized water (dI) or a hydrogen peroxide standard was pipetted through the cap hole. The tape was replaced and the vial briefly inverted to ensure that no peroxide remained uncombined with the DCFH solution. The vials were incubated in a 37 °C water bath for 15 min. The solution was then briefly agitated by hand and placed in line with the analytical system, shown in Fig. 1. A peristaltic pump moved the DCFH-HRP-H₂O₂ solution at 0.4 mL min⁻¹ through the flow-through cell, while a selector valve directed dI through the cell when not measuring DCFH intensity. A small glass debubbler was also employed to reduce the signal interference by small air bubbles that may be introduced into the system, also run from the peristaltic pump. Volume loss from the discarded flow was approximately 10 % of the overall sample flow. Sufficient dI was allowed to move through the system to return the fluorescent signal to a baseline value before analyzing the next sample. The entire system was plumbed with green PEEK tubing (1/16" outer diameter, 0.030" inner diameter, Upchurch Scientific, Oak Harbor, WA, USA).

As the solution moved through the flow cell, it was excited by the 475 nm light source, causing the DCF* product to fluoresce at 530 nm. This light intensity is transmitted via the fiber optic cable to the spectrophotometer. Fluorescent intensity at 530 nm was measured using SpectraSuite from Ocean Optics and recorded with an integration time of 500 ms and average of 10 scans. Prior to any analysis a dark spectrum signal was measured while blocking all light to the spectrometer and subtracted automatically from the light spectrum. Intensity values reported are average intensities of measurements made once the fluorescent signal was stabilized, after a minimum of 10 min from powering on the excitation source. Deionized water also provided a measurable signal

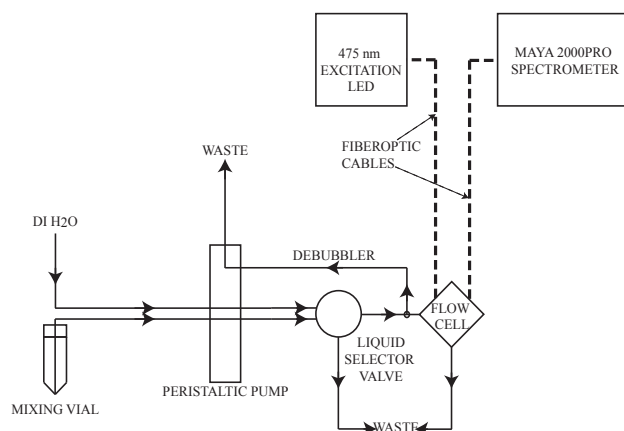


Fig. 1. Schematic for offline ROS analysis of standards and reagents combined in a mixing vial. DCFH + ROS (H₂O₂ for calibrations) is pumped via the peristaltic pump through the flow cell, in which the concentration of DCF is measured at 530 nm by the spectrometer. A selector valve switches between sample and deionized water to provide a baseline and to clear out the flow cell between samples.

at 530 nm, which was used as a surrogate for light source intensity and system flow stability over time.

An example of an initial calibration made with H₂O₂ solution concentrations of 100–400 nM is shown in Fig. 2. This sample range was chosen as a representative span for the concentrations reported in ROS_p analysis for typical filter measurement setups (Hung and Wang, 2001; Venkatachari et al., 2005, 2007).

3.2 Offline sensitivity analysis

Previous work has reported the need to control the DCFH-HRP working solution storage temperature, storage time (solution age), pH, and operational parameters including reaction temperature, pH and reaction time to achieve maximum reaction of DCFH with hydrogen peroxide. Parameters were optimized to reduce auto-oxidation and thus lengthen the usable lifespan of the DCFH-HRP solution, hereafter referred to as working solution (Cathcart et al., 1983; Black and Brandt, 1974), and to provide the greatest method response. Parameters were assessed primarily by comparing hydrogen peroxide calibration slopes relative to the base case, previously described. DCFH age was examined by comparing the calibration slope of a fresh solution with the calibration slope hours and days later. Reaction temperature was assessed by comparing calibration slopes of solutions incubated at varying temperatures from ambient (23 °C) to 65 °C prior to analysis. A similar method of assessment was used to determine the optimal DCFH concentration and DCFH : sample volumetric ratios (e.g., the ratio of the volume of working solution to the volume of calibration standard). A 30 : 1 ratio, used for the base case, was not considered practical for a future online system. Finally, reaction time was assessed using

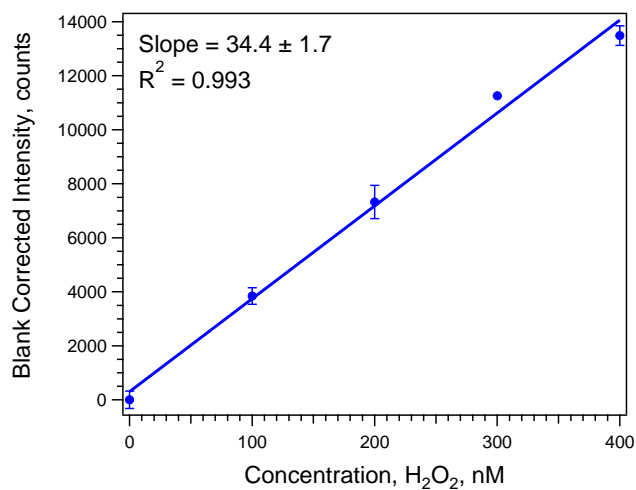


Fig. 2. Calibration of offline ROS assay using DCFH with known concentrations of H₂O₂. Error bars represent the standard deviation of multiple measurements ($n = 5$).

a different setup in order to measure reaction progress. In those tests, 0.1 mL of a hydrogen peroxide standard or DI was pipetted into the mixing vials as described previously with 3 mL of DCFH solution, briefly inverted to ensure that all liquids were combined and immediately placed in line with the detector. The sample line from vial to detector was shortened as much as possible to reduce delay time from which DCFH and peroxide were combined to initial detection of fluorescence, using the same 0.030" ID PEEK tubing as in the standard flow analysis setup from Fig. 1. The residence time in line prior to detection was 30 s. The findings from these offline assessments are summarized in Table 1 and used in the application of the online instrument.

4 Online instrument development

4.1 Mist chamber

Originally known as the Cofer scrubber, mist chambers were developed to collect water soluble gases and particles for online analysis (Cofer III et al., 1985, 1986; Anderson et al., 2008; Spaulding et al., 2002). Mist chambers are generally a cylindrical glass structure with an air sample inlet at the bottom, a port on the side for introduction and removal of scrubbing liquids, and a nebulizing nozzle, as shown in Fig. 3. Sample air enters the chamber through the bottom nozzle. Inside the chamber, a capillary runs from just above the base and alongside the air nozzle for some vertical distance. Some minimum volume of liquid, usually water, is placed inside the mist chamber via the injection port. Venturi forces created by the airflow accelerate through the nozzle, draw liquid from the reservoir into the airstream and create a fine mist. Affixed to the top of the mist chamber is a

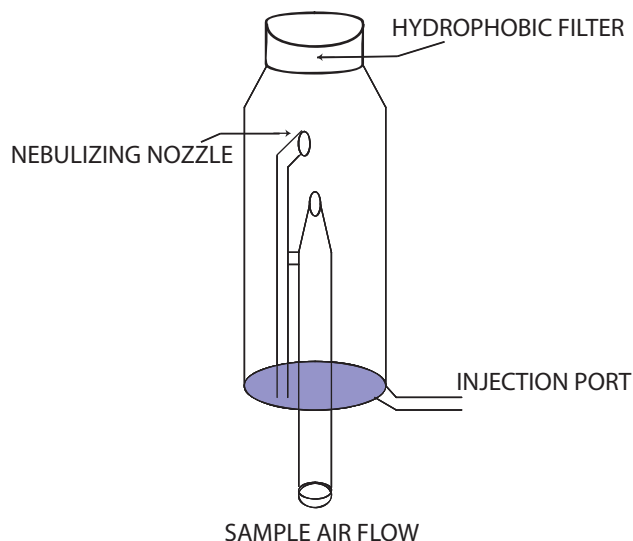


Fig. 3. Schematic of a mist chamber. Liquid is injected and extracted via the port at the bottom of the chamber. Sample air is drawn through the opening in the base of the chamber, nebulizing the liquid inside and creating a mist of droplets. Liquids are retained by means of a hydrophobic filter attached to the top of the mist chamber, which also refluxes liquid back down the sides of the glass.

Table 1. Optimal parameters for use in online instrumentation.

Parameter	Value
Maximum viable DCFH useful age	2 days
Reaction temperature	ambient
DCFH concentration	10 μ M
Volumetric ratio	Arbitrary (9 : 1–30 : 1)
Minimum reaction time	3 min

filter pack (University Research Glassware (URG), Carrboro, NC, USA) equipped with a 1.0 μ m pore size hydrophobic filter (TefSep, Pall Corporation). This filter prevents the liquid from exiting the chamber, which refluxes down from the top of the mist chamber back to the reservoir. This liquid scrubs the soluble gases and particles from the airstream as it is continually recycled through the chamber. Some liquid is inevitably lost as water vapor in the exhaust flow. When sample airflow is halted, the liquid and its components in solution are withdrawn from the chamber for analysis. Analysis of the sample can occur while the next mist chamber sampling cycle starts.

Benefits of the mist chamber include operation without heating the sample and the ability to vary integration time in order to concentrate samples. The mist chamber has been shown to effectively collect compounds with a Henry's law constant, K_H , of over 10^3 M atm^{-1} (Spaulding et al., 2002). The potential drawbacks of the system include the need for a batch operation process, which tends to consume

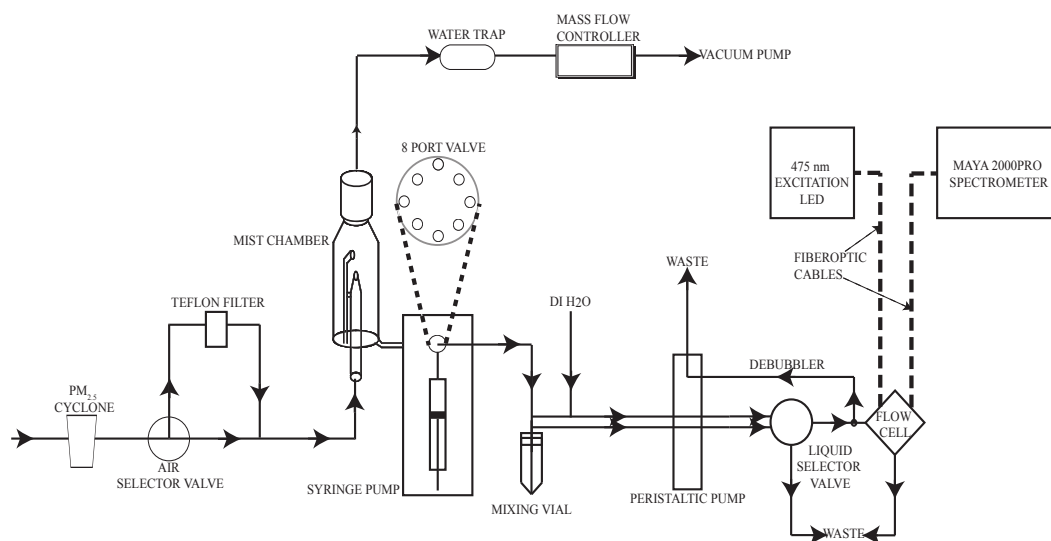


Fig. 4. Schematic of online $\text{PM}_{2.5}$ ROS measurement approach using a mist chamber particle collection system and fluorometric probe.

more water as opposed to a continuous monitoring system. Mist chambers are also effective scrubbers of gases, unlike condensation-based systems, indicating the need for an effective gas phase control to effectively measure solely particle concentrations. A mist chamber was chosen as the particle collection for the online ROS_p instrument in part due to control of sample integration times to overcome analytical detection limits.

4.2 Online method setup

The overall setup of the mist chamber-based ROS instrument is shown in Fig. 4. Ambient air is drawn through a cyclone ($\text{PM}_{2.5}$, 16.7 L min^{-1} , URG) and a copper inlet line. The air flow enters an automated valve that either directs it through a 47 mm filter pack (URG) containing a $2.0 \mu\text{m}$ Teflon filter (Zefluor, Pall Corporation) for measurements of ROS_g , or bypasses the filter for a measurement of $\text{ROS}_g + \text{ROS}_p$, or total ROS (ROS_t). The sample air then enters the mist chamber, after which the scrubbed airstream exits through the hydrophobic filter. The airflow finally passes through a water trap followed by a mass flow controller (GFC-47, Aalborg), set nominally at 20 L min^{-1} , and then to a vacuum pump (carbon vane, Gast 1/4 hp). These sampling system components were specifically chosen to maximize retention of $\text{PM}_{2.5}$ and thus ROS_p .

A syringe pump equipped with an 8-port valve (V6 pump with 48 K resolution, Norgren Kloehn, Las Vegas, NV, USA) and a continuously operating peristaltic pump (4-channel, Ismatec) control the liquid portion of the instrument. One port of the syringe pump is connected to the mist chamber liquid inlet; the other ports led to a reservoir of the DCFH-HRP working solution, DI, waste, and a 15 mL amber centrifuge tube (mixing vial) as described in the offline analysis method.

The remaining three ports can be used for up to two hydrogen peroxide standards for automatic calibrations, and for an open port for introduction of air, as required. The V6 pump also electronically controls the power to the vacuum pump through a solid-state relay as well as the position of the sample air selector valve and a two-position liquid selector valve to change the source of the liquid flow into the flow cell.

The peristaltic pump continuously moves liquid from either the mixing vial or the DI reservoir through the flow cell. This amber mixing vial contains two PEEK tubing lines inserted through the hole in the cap. The line from the peristaltic pump extended to the vial bottom while the line from the syringe pump valve extended only a short distance past the cap. This setup allows for all liquid to be withdrawn completely via the longest line from the mixing vial, while the shorter line does not reach the liquid level within the vial at any time. A third channel on the peristaltic pump also controls flow from a glass debubbler in line just prior to the flow-through cell. The fourth channel drains liquid from the water trap to protect the mass flow controller. The syringe and all other clear portions of this system are shielded from light with aluminum foil to inhibit photooxidation of the DCFH.

4.3 Sampling automation and analysis

The following describes a typical sample collection and analysis cycle using a looping routine in the syringe pump (Kloehn Control) software. The start of the sampling cycle begins with the syringe pump injecting 10 mL of DI into the mist chamber. The vacuum pump is started for a period of 5 min to collect soluble ROS ambient species in the mist chamber collection liquid. The vacuum pump is shut off, and the syringe pump withdraws 1.5 mL of the ROS-laden solution from the mist chamber; 0.5 mL of this from the top of the

syringe is immediately discarded to remove any air from the liquid system. A total of 9 mL of working solution are then added to the syringe. The combined total 10 mL of sample liquid and working solution is forced into the mixing vial via the higher level tube. This process mixes the sample of dissolved ROS components and working solution. During this time, the peristaltic pump is running continually, pumping dI through the flow cell and the mixed sample-reagent solution from the vial is sent to waste, until after 1 min, at which point the vial liquid has reached the selector valve, which then is actuated to direct vial liquid to the flow cell (dI now to waste). The reacted sample solution moves through the flow cell for 2.5 min, at the end of which the fluorescent signal is recorded. This results in a fluorescent signal quantified after 4.5 min of reaction time. Deionized water in between samples provides a baseline as previously discussed.

During the analysis of the ambient sample by the spectrometer, the syringe pump cleans the mist chamber prior to reloading it for another sample by draining and discarding the remaining sample liquid. Water used for sample collection is added to the mist chamber. The air selector valve is adjusted to filter ambient air and the vacuum pump runs for 30 s, rinsing the mist chamber with particle-free air and water (but does contain ambient ROS_g). The vacuum pump is shut off, and this water withdrawn and discarded.

After the final measurements of the fluorescent signal, the liquid selector valve returns to its prior state, pumping any remaining sample from the mixing vial to waste and rinsing the flow cell with dI. The syringe pump then also withdraws and discards remaining sample solution to completely empty the vial and flushes the vial once with dI.

Since part of the analysis time includes preparing the mist chamber for the next measurement, there is a delay of 5.5 min between sampling cycles. For example, one complete cycle of the general ROS sampling and analysis cycle takes 10.5 min when collecting sample in the mist chamber for 5 min. Longer duty cycles were employed when the mist chamber sample collection time was increased to produce more concentrated samples.

4.4 Mist chamber particle collection efficiency and liquid loss

The mist chamber was constructed by the department glass blower, so variation between different chambers is possible. This variation and the subsequent potential operational collection efficiency differences must be evaluated. Collection efficiencies were determined by comparing the collection of sulfate with a simultaneous operation of the PILS-IC system (Orsini et al., 2003). The ROS instrument was operated entirely in ROS_t mode and fitted with a gas denuder upstream. The collected liquid was drawn from the mist chamber into a vial, which was then analyzed manually by the same IC measuring the sample collected by the PILS. Multiple measurements of ambient PM_{2.5} sulfate concentrations

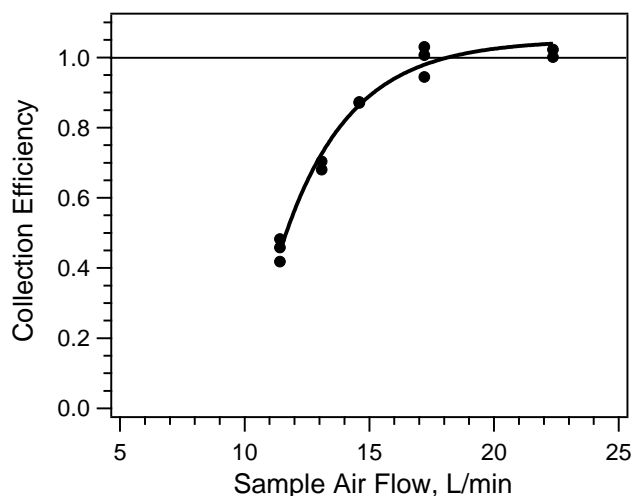


Fig. 5. Mist chamber collection efficiency. Collection efficiency determined by ratio of ambient sulfate measured with the mist chamber-IC to that from a PILS-IC system.

were conducted at different mist chamber sample airflow rates. The resulting collection efficiency (mist chamber sulfate to PILS sulfate) shown in Fig. 5 shows that this specific mist chamber should be operated at a minimum flow rate of 15 L min⁻¹. Maximum flow rates for this particular setup were limited to approximately 25 L min⁻¹ due to pressure drop across various elements of the system, mainly from the wetted hydrophobic refluxing filter.

While the refluxing hydrophobic filter that retains liquid in the mist chamber is effective, inevitably some liquid loss occurs. The final volume of liquid retained by the mist chamber is measured periodically to account for this loss to account and to determine the ambient concentration. This potential loss was also a motivating factor in the short sampling periods employed during the majority of the instrument's field deployment.

4.5 Online calibration and dynamic liquid blanks

The ROS instrument is calibrated with the mist chamber offline in an automated process using the analytical system just described. Instead of liquid from the mist chamber being combined with the DCFH working solution in the mixing vial, the same volume of a standard is used. This allows the verification of known concentrations as part of routine operation. "Blank", or auto-oxidation, measurements to adjust for working solution age and subsequent increase in baseline fluorescent intensity were also made using dI. Figure 6 shows a typical plot from such a calibration, using standard concentrations in the range anticipated for ambient sampling with the online instrument.

As "blank" measurements in this system are truly measurements of the auto-oxidation state of the working solution, they must be measured regularly during the sampling

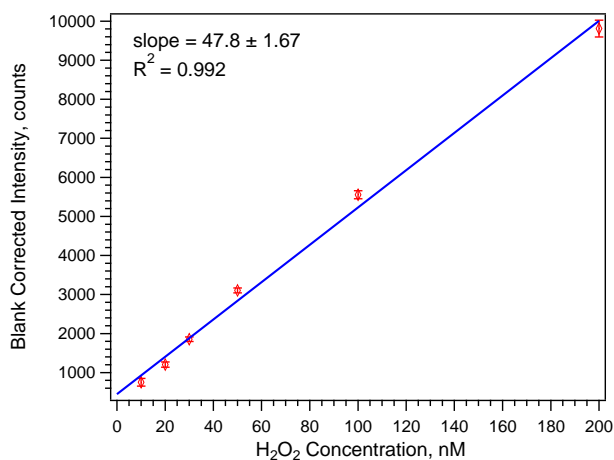


Fig. 6. Calibration of online ROS assay using DCFH with known concentrations of H_2O_2 . Error bars represent the standard deviation of multiple measurements ($n = 5$).

operation to allow for dynamic correction of the sample fluorescent signal over time. The blank signal is measured after every 6 ambient measurements, or approximately every hour. Figure 7 shows a sample of the drift over roughly a 48 h sample period of the blank signal during field-testing of the instrument.

4.6 Calculation of ambient ROS concentration

The ROS concentration in the ambient air in H_2O_2 equivalents is calculated by

$$C_a = \left(\frac{I - b}{a} \right) \left(\frac{V_s}{1000 Q_{at}} \right) 1000 \text{ L m}^{-3}, \quad (1)$$

where I is the intensity of the fluorescent signal (counts), b the intercept from calibration linear fit, a the slope from calibration linear fit, V_s final solution volume (mL) in mist chamber, and Q_a the average airflow through the mist chamber (L min^{-1} , ambient T and p) for a sampling period of t (min). Multiplying C_a by 1000 L m^{-3} results in an ambient ROS concentration in $\text{nmol H}_2\text{O}_2$ equivalents m^{-3} .

4.7 Evaluation of gas phase removal and ROS_p calculation by difference

Several compounds were assessed as dry scrubbers or as annular denuder coatings for use in ROS_g removal to improve determination of ROS_p . A glass annular denuder (URG) coated with a slurry of MnO_2 and a diffusion dryer filled with Carulite (a dry MnO_2 compound) (Carus Corporation, Peru, IL, USA) were evaluated for their ability to remove ROS_g . MnO_2 was of primary interest since this has been an ROS removal compound used in previous studies (Hwang and Dasgupta, 1986; Stobbe et al., 1999). Ti(IV) oxalate was also used in an annular denuder coating, given its use in scrubbing

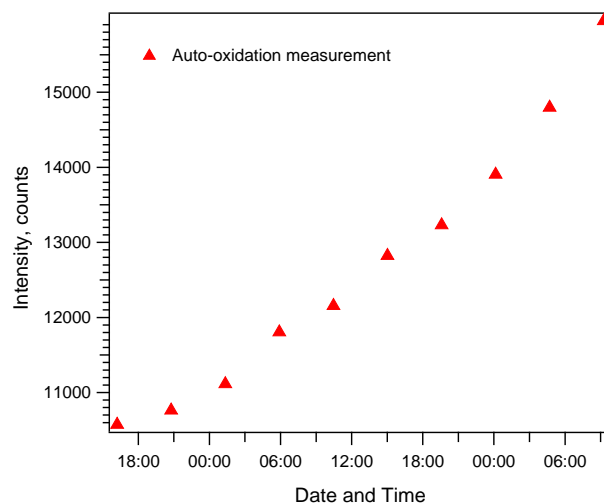


Fig. 7. Auto-oxidation (pure water blank) measurements of DCFH over time, demonstrating the drift of the DCFH working solution during regular operation of the online instrument.

hydrogen peroxide (Possanzini et al., 1988; Possanzini and Di Palo, 1995).

Denuder efficiency tests were done by consecutive denuder-on versus denuder-bypass ROS measurements with the automated mist chamber system by placing the Teflon filter upstream of the complete system, and the denuder in the position formerly occupied by the filter controlled by the air selection valve. The annular denuder coated with a MnO_2 slurry removed an average of 9 % of the ambient ROS_g , with a maximum removal efficiency of 57 % (standard deviation of removal efficiency was 21 % ($n = 111$)). Dry MnO_2 packed into the diffusion dryer removed an average of 18 %, with a maximum of 39 % and a standard deviation of 11 % ($n = 113$). Ti(IV) oxalate denuders were evaluated for a briefer period of time, with an average removal efficiency of 12 % and a standard deviation of 33 % ($n = 24$).

Tests were also performed to determine if there were ROS_g interferences from ozone. Measurements from sampling laboratory-generated ozone at concentrations between 60 and 180 ppb showed little response, as expected given its low solubility (K_H of 0.011 M atm^{-1}) (Kosak-Channing and Helz, 1983).

The low removal efficiency and high variability suggested that these denuders would not be effective in removing ROS_g consistently enough to include in a system that depended on reliable gas removal for artifact-free measurements. This conclusion led to the regular use of the difference method for determining ROS_p from ROS_t and ROS_g , measured in an alternating fashion. ROS_p in $\text{nmol H}_2\text{O}_2$ equivalents m^{-3} was determined by

$$\text{ROS}_{p,i} = \frac{[\text{ROS}_{t,i} - \text{ROS}_{g,i-1}] + [\text{ROS}_{g,i} - \text{ROS}_{g,i+1}]}{2}, \quad (2)$$

where i represents the number in the series of consecutive ROS measurements.

4.8 Precision and limits of detection

Precision was determined by the standard deviation of a repeated standard in a calibration setting and the periodic measurement of standards during routine field operation of the instrument. The analytical precision based on repeated calibration standards was 6.2%, $n = 30$ (1.26 nM liquid concentration, or under normal operating parameters, 0.025 nmol H₂O₂ equivalents m⁻³). Precision of the field-deployed instrument, based on periodic measurements of standards during routine operation, was 7.1% ($n = 10$).

The limit of detection for measuring ROS considering just the analytical portion of the method was determined by three times the standard deviation of the blank measurements made in succession (DCFH working solution and dI). The resulting liquid concentration limit of detection was 0.28 nM H₂O₂ equivalents, or 0.029 nmol H₂O₂ equivalents m⁻³ for the normal operational values of the mist chamber, in which the final liquid volume is 9.7 mL, airflow rate 20 L min⁻¹ and the sample collection time 5 min. For the field-deployed instrument, ROS measurement limit of detection (LOD) was similar for consecutive blanks.

The method LOD for determining ROS_p is substantially higher, however, since it involves a difference between two large values of relatively close magnitude. During the field measurements described below, frequent negative ROS_p values resulted from the difference calculation. An alternate and conservative LOD was used based on the variability in the negative ROS_p values. For example, once ROS_p was determined for a specific study period (e.g., a specific site) and after basic quality control removed erroneous measurements of erratic highs or lows, the LOD for the particle measurements was estimated from one standard deviation of all negative values calculated from the difference method. The calculated LOD by this method varied between 0.07 and 0.19 nmol H₂O₂ equivalents m⁻³, with an average value of 0.15 nmol H₂O₂ equivalents m⁻³. The high LOD associated with this difference method emphasizes the importance of reducing or eliminating the gas signal from the particle measurement. Future progress is needed in this area to improve the ROS_p method used in this work.

5 Results and discussion

5.1 Field deployment

The ROS mist chamber was evaluated for ambient sampling by deployment at a number of sites during various seasons. Sites included the Southeastern Aerosol Research and Characterization (SEARCH) network Jefferson Street site (JST) from 7 February to 2 March 2012, and 8 May to 31 May 2012. Located in central urban Atlanta, GA, the site is considered representative of urban Atlanta (Hansen et al., 2006). Measurements were made at Yorkville

Table 2. Comparison of average and span of online ROS_p measurements during summer study period.

Month/Location	ROS _p Mean (nmol H ₂ O ₂ equivalents m ⁻³)	Total No. of Measurements below LOD	Range	Standard Deviation
May 2012 (JST) ($N = 998$)	0.26 ± 0.013	725	0.04–2.74	0.33
June 2012 (YRK) ($N = 439$)	0.14 ± 0.0091	351	0.07–1.95	0.19
July 2012 (GT) ($N = 512$)	0.24 ± 0.010	128	0.15–2.97	0.29

(YRK), the SEARCH rural pair to JST located approximately 80 km northwest of Atlanta, 8 June to 29 June 2012. Finally, measurements were made from the rooftop monitoring site at Georgia Tech (GT) (midtown Atlanta), 3 July to 31 July 2012, a site more impacted by highway traffic emissions than the JST site.

An example of the type of raw data produced by the instrument is shown in Fig. 8. The time series of the fluorescent intensity at 530 nm shows a series of peaks starting from a baseline of roughly 6000 counts. Adjustments were made on a weekly basis to maintain the baseline intensity at this level as a surrogate for controlling LED output intensity and to create consistent excitation in the samples. Peak heights are the response to measurements when the DCFH working solution is mixed with either a dI “blank”, a standard, or a mist chamber sample of ROS_i or ROS_g. ROS measurements and calibration standards are corrected by subtracting an estimated “blank” determined from a linear interpolation between successive auto-oxidation measurements. In this example, a set of 8 ROS measurements were made by alternating between ROS_i and ROS_g between blanks or standards. Standards are less frequently analyzed than blanks.

During May (JST) and June (YRK), the ROS instrument was operated using a 5 min sampling period, but increased to 30 min for later portions of the GT July study. Figure 9 shows the time series of ROS_p measured at the Georgia Tech site. Table 2 provides a statistical summary of ROS_p concentrations from each site. The ambient results are discussed following a comparison between the online system and filter measurements.

5.2 Comparison with filter concentrations

A short ROS_p-filter study was conducted in order to compare online ROS_p concentrations to the more traditional methods used to date. This comparison study was conducted in July 2012 while the instrument was deployed at the Georgia Tech site. Over a period of 16 weekdays, 1 μm polycarbonate filters (Nuclepore, Whatman) were loaded with PM at an average flow rate of 45 L min⁻¹. Measurements were made of total suspended particulate matter; no size selector was used so that the filter flow rate could be maximized. To minimize sampling artifacts, sampling times were kept short, typically

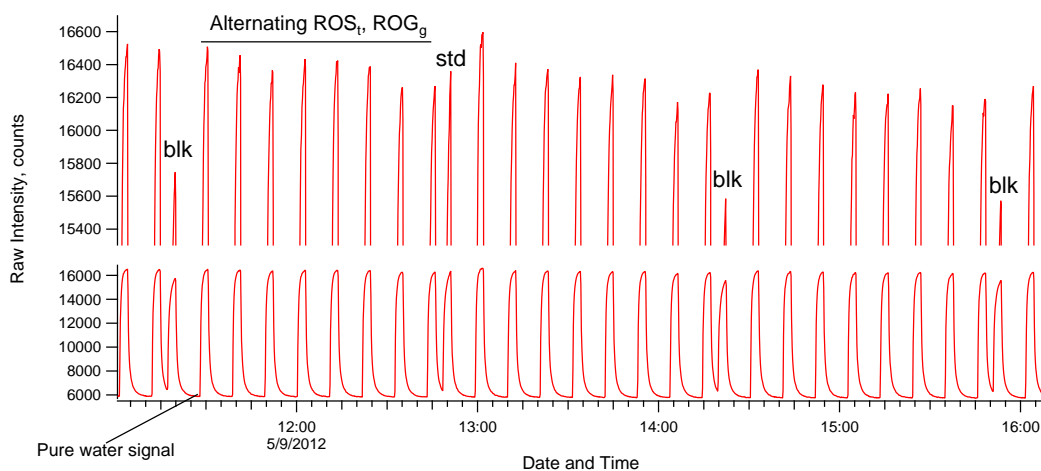


Fig. 8. Time series of raw spectrometer data for ambient ROS measurements showing responses for pure water, deionized water + DCFH/HRP (blk), online measurements of total and gas ROS, and H_2O_2 standards (std).

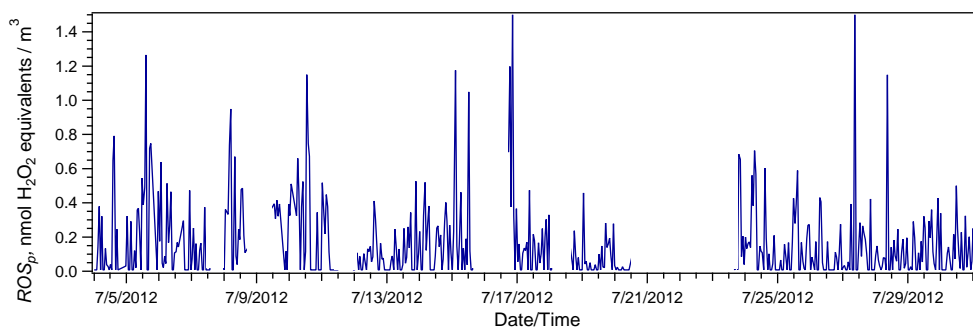


Fig. 9. Time series plot of ROS_p at the Georgia Tech sites. ROS_p below estimated limit of detection is plotted as $0.5 \cdot (\text{LOD})$.

3 h. Following sampling, filters were immediately extracted into 30 mL of the same batch of DCFH working solution being used in the co-located online instrument, mechanically shaken using a wrist-action shaker (mechanical wrist action shaker, Model 70, Burrell Scientific, Pittsburgh, PA, USA) for 15 min and analyzed using an identical setup to the online system. This procedure deviated from other studies' filter measurements (Hung and Wang, 2001) in two ways: one, the same volume of DCFH was used for each filter, and, two, filters were shaken rather than sonicated to extract the particles into solution. Filter blanks and water blanks were also measured and standards were checked routinely.

Since the majority of the online measurements were comprised of values at or below the LOD, only average comparisons are made between the filter and online ROS_p . No filter measurement was below the filter LOD ($0.016 \text{ nmol H}_2\text{O}_2 \text{ equivalents m}^{-3}$). In cases where measurements were below the LOD, $1/2 \text{ LOD}$ was used in the statistical calculations. Results from the filter comparison are detailed in Table 3. The filter measurements tend to agree with the online results, despite the fact the filters were TSP and the online method sampled $\text{PM}_{2.5}$. The average filter

Table 3. Comparison of online and offline ROS_p measurements, 12–27 July 2012.

Method	ROS_p Mean ($\text{nmol H}_2\text{O}_2$ equivalents m^{-3})	Range	Standard Deviation
Online (mist chamber)	0.16 ± 0.010	0.01–0.70	0.17
Offline (filters) ($N = 19$)	0.15 ± 0.019	0.05–0.34	0.079

ROS_p was $0.15 \text{ nmol H}_2\text{O}_2 \text{ equivalents m}^{-3}$ compared to 0.16 nmol m^{-3} for the online system. The online data are largely driven by adjustments made for values below the LOD. This agreement suggests that the online measurement methods employed during this study are as effective as making careful yet rapid filter (e.g., highly labor-intensive) measurements of ambient ROS.

Table 4. Summary of ROS_p studies.

Location	Dates	Concentration (nmol m ⁻³)	Reference
Flushing, NY	Jan–Feb 2004	0.87 ± 0.18	Venkatachari et al. (2007)
Singapore (roadway)	Dec 2005	15.10 ± 0.10	See et al. (2007)
Singapore (ambient)	Dec 2005	5.71 ± 2.30	See et al. (2007)
Taipei (Taiwan)	Jul–Dec 2000	0.54 ± 0.40	Hung and Wang (2001)
Rubidoux, CA	Jul 2003	5.90 ± 1.70	Venkatachari et al. (2005)
Rochester, NY	Aug 2009	8.30 ± 2.19	Wang et al. (2011)
Atlanta, GA (online)	May, Jul 2012	0.25 ± 0.01	This study
Atlanta, GA (filters)	Jul 2012	0.15 ± 0.019	This study

6 Discussion of online field results

Both urban sites (JST and GT) showed significantly higher ROS_p concentrations when compared with the rural site (YRK) ($p < 0.001$ and $p < 0.05$ respectively). The JST and GT mean ROS_p concentrations were also different ($p < 0.001$) at 0.26 and 0.24 nmol H₂O₂ equivalents m⁻³, respectively, whereas YRK was roughly half that at 0.14 nmol H₂O₂ equivalents m⁻³. These numbers are uncertain since much of the data were below the LOD of 0.15 nmol m⁻³, but the urban sites had fewer values below LOD, consistent with generally higher ROS_p values.

The GT location is much closer to a congested 16-lane highway that runs through the middle of the city. Online measurements of elemental carbon (EC), a tracer for primary aerosol, show a greater influence of roadway emissions at GT. For example, GT/JST EC ratio was 1.36 for July 2012. This comparison, though, is somewhat ambiguous since the ROS_p measurements made at the two sites were at different times (JST in May 2012, GT in July 2012), but still no large difference is observed for a site expected to be more impacted by highway emissions. The lower concentrations at the rural site suggest urban emission may be related to ROS_p.

These offline and online measurements of ROS_p are generally lower than what has been reported by other investigators, as summarized previously (Wang et al., 2011) and shown in Table 4. Filter-based studies have reported ROS_p concentrations in the range of 0.54 to 15.1 nmol H₂O₂ equivalents m⁻³, about an order of magnitude above levels measured in this study. The few online studies conducted over much shorter time periods (1 week) report a mean ROS_p concentration of 8.30 ± 2.19 nmol m⁻³ (Wang et al., 2011). The highest concentrations are found in studies conducted next to roadways, possibly suggesting that extremely fresh emissions from these locations can lead to higher measured concentrations. It is not clear why the concentrations in Atlanta and vicinity are significantly lower. This could be due to different emission characteristics, linked to different measurement methods, or due to some of the substantial challenges associated with using this chemical probe.

7 Conclusions

An automated flow system and online instrument was developed for analysis of ROS using a mist chamber collection system coupled to an analytical system employing DCFH as a fluorescent probe. The system was operated using a set of operational parameters optimized based on extensive laboratory experiments. The analytical system LOD was 0.28 nM. This detector was coupled to a mist chamber for collecting and concentrating ROS components in water. PM_{2.5} ROS (ROS_p) was determined by the difference between total gas plus particle (ROS_t) and filtered air (i.e., gas-phase ROS, ROS_g). This method was chosen since experiments with various denuders showed low and variable effectiveness for removing ROS_g. Higher LODs are associated with this method versus potential direct online methods due to high ROS_g levels relative to ROS_p. For the three months of measurements reported in this study, the percentage of ROS_g to total ROS_g/ROS_t was 96 ± 124 % (one standard deviation). Online measurements were above the detection limit of nominal 0.15 nmol H₂O₂ equivalents m⁻³ approximately 25 % of the time. ROS_g artifacts can be reasonably expected to dominate other liquid-based systems. During the field deployment of the instrument, concentrations of ROS_p were higher in urban areas relative to a rural site, averaging 0.25 nmol H₂O₂ equivalents m⁻³ for urban Atlanta in May and July, versus 0.14 nmol H₂O₂ equivalents m⁻³ at the rural Yorkville site during June. These online results were consistent with a series of filter samples using the same ROS analytical system designed for the online method. The ROS_p reported in this study is significantly below what has been reported by other investigators, with ranges between 0.54 and 15.1 nmol H₂O₂ equivalents m⁻³. Application of the DCFH probe to measurement of ambient particle ROS is challenging due to a number of factors, including auto-oxidation of the working solution over a short period of time as well as photosensitivity and potential for large interferences from ROS_g.

Acknowledgements. This research was made possible through USEPA grant R834799. The contents of this paper are solely the responsibility of the grantee and do not necessarily represent the official views of the USEPA. Further, USEPA does not endorse the purchase of any commercial products or services mentioned in the publication. This research was also made possible in part by collocating field deployments with sites operated by Atmospheric Research and Analysis (ARA) as part of the Southeastern Aerosol Research and Characterization (SEARCH) network of monitoring stations, which are funded in part by the Electric Power Research Institute (EPRI) and the Southern Company. This work does not necessarily represent the views of any of the above parties, nor do they endorse any of the commercial products mentioned within this text.

Edited by: P. Herckes

References

- Anderson, C. H., Dibb, J. E., Griffin, R. J., Hagler, G. S. W., and Bergin, M. H.: Atmospheric water-soluble organic carbon measurements at Summit, Greenland, *Atmos. Environ.*, 42, 5612–5621, doi:10.1016/j.atmosenv.2008.03.006, 2008.
- Antonini, J. M., Clarke, R. W., Murthy, G. G. K., Sreekantham, P., Jenkins, N., Eagar, T. W., and Brain, J. D.: Freshly generated stainless steel welding fume induces greater lung inflammation in rats as compared to aged fume, *Toxicol. Lett.*, 98, 77–86, 1998.
- Barrett, W. C., DeGnoro, J. P., Keng, Y.-F., Zhang, Z.-Y., Yim, M. B., and Chock, P. B.: Roles of Superoxide Radical Anion in Signal Transduction Mediated by Reversible Regulation of Protein-tyrosine Phosphatase 1B, *J. Biol. Chem.*, 274, 34543–34546, 1999.
- Black, M. J. and Brandt, R. B.: Spectrofluorometric Analysis of Hydrogen Peroxide, *Anal. Biochem.*, 58, 246–254, 1974.
- Cathcart, R., Schwiers, E., and Ames, B. N.: Detection of Picomole Levels of Hydroperoxides Using a Fluorescent Dichlorofluorescein Assay, *Anal. Biochem.*, 134, 111–116, 1983.
- Cofer III, W. R., Collins, V. G., and Talbot, R. W.: Improved Aqueous Scrubber for Collection of Soluble Atmospheric Trace Gases, *Environ. Sci. Technol.*, 19, 557–560, 1985.
- Cofer III, W. R., Edahl, J., and Robert A.: A New Technique For Collection, Concentration and Determination of Gaseous Tropospheric Formaldehyde, *Atmos. Environ.*, 20, 979–984, 1986.
- Cohn, C. A., Simon, S. R., and Schoonen, M. A. A.: Comparison of fluorescence-based techniques for the quantification of particle-induced hydroxyl radicals, *Particle and fibre toxicology*, 5, 2, doi:10.1186/1743-8977-5-2, 2008.
- Hansen, A., Edgerton, E., Hartsell, B., Jansen, J., Burge, H., Koutrakis, P., Rogers, C., Suh, H., Chow, J., Zielinska, B., McMurry, P., Mulholland, J., Russell, A., and Rasmussen, R.: Air Quality Measurements for the Aerosol Research and Inhalation Epidemiology Study, *J. Air Waste Manage. As.*, 56, 1445–1458, 2006.
- Hung, H.-F. and Wang, C.-S.: Experimental determination of reactive oxygen species in Taipei aerosols, *J. Aerosol Sci.*, 32, 1201–1211, 2001.
- Hwang, H. and Dasgupta, P. K.: Fluorometric flow injection determination of aqueous peroxides at nanomolar level using membrane reactors, *Anal. Chem.*, 58, 1521–1524, doi:10.1021/ac00298a055, 1986.
- Kao, M.-C. and Wang, C.-S.: Reactive Oxygen Species in Incense Smoke, *Aerosol Air Quality Res.*, 2, 61–69, 2002.
- Klippel, T., Fischer, H., Bozem, H., Lawrence, M. G., Butler, T., Jöckel, P., Tost, H., Martinez, M., Harder, H., Regelin, E., Sander, R., Schiller, C. L., Stickler, A., and Lelieveld, J.: Distribution of hydrogen peroxide and formaldehyde over Central Europe during the HOOPER project, *Atmos. Chem. Phys.*, 11, 4391–4410, doi:10.5194/acp-11-4391-2011, 2011.
- Kosak-Channing, L. F. and Helz, G. R.: Solubility of Ozone in Aqueous Solutions of 0–0.6 M Ionic Strength at 5–30 C, *Environ. Sci. Technol.*, 17, 145–149, 1983.
- LeBel, C. P., Ischiropoulos, H., and Bondy, S. C.: Evaluation of the Probe 2',7'-Dichlorofluorescein as an Indicator of Reactive Oxygen Species Formation and Oxidative Stress, *Chem. Res. Toxicol.*, 5, 227–231, 1992.
- Lee, J. H., Chen, Y., and Tang, I. N.: Heterogeneous Loss of Gaseous H₂O₂ in an Atmospheric Air Sampling System, *Environ. Sci. Technol.*, 25, 339–342, 1991.
- Liu, H. H., Wu, Y. C., and Chen, H. L.: Production of ozone and reactive oxygen species after welding, *Archives of environmental contamination and toxicology*, 53, 513–518, doi:10.1007/s00244-007-0030-1, 2007.
- Morgan, T. E., Davis, D. A., Iwata, N., Tanner, J. A., Snyder, D., Ning, Z., Kam, W., Hsu, Y.-T., Winkler, J. W., Chen, J.-C., Peta-sis, N. A., Baudry, M., Sioutas, C., and Finch, C. E.: Glutamatergic Neurons in Rodent Models Respond to Nanoscale Particulate Urban Air Pollutants In Vivo and In Vitro, *Environ. Health Persp.*, 119, 1003–1009, 2001.
- Oberdörster, E.: Manufactured Nanomaterials (Fullerenes, C₆₀) Induce Oxidative Stress in the Brain of Juvenile Largemouth Bass, *Environ. Health Persp.*, 112, 1058–1062, doi:10.1289/ehp.7021, 2004.
- Orsini, D. A., Ma, Y., Sullivan, A., Sierau, B., Baumann, K., and Weber, R. J.: Refinements to the particle-into-liquid sampler (PILS) for ground and airborne measurements of water soluble aerosol composition, *Atmos. Environ.*, 37, 1243–1259, doi:10.1016/s1352-2310(02)01015-4, 2003.
- Pope, C. A., Thun, M. J., Namboodiri, M. M., Dockery, D. W., Evans, J. S., Speizer, F. E., and Heath, C. W.: Particulate air pollution as a predictor of mortality in a prospective study of US adults, *Am. J. Resp. Crit. Care*, 151, 669–674, 1995.
- Possanzini, M. and Di Palo, V.: Improved titanium method for determination of atmospheric H₂O₂, *Anal. Chim. Acta*, 315, 225–230, 1995.
- Possanzini, M., Di Palo, V., and Liberti, A.: Annular denuder method for determination of H₂O₂ in the ambient atmosphere, *Sci. Total Environ.*, 77, 203–214, 1988.
- Reeves, C. E. and Penkett, S. A.: Measurements of Peroxides and What They Tell Us, *Chem. Rev.*, 103, 5199–5218, 2003.
- Rothe, G. and Valet, G.: Flow Cytometric Analysis of Respiratory Burst Activity in Phagocytes with Hydroethidine and 2',7'-Dichlorofluorescein, *J. Leukocyte Biol.*, 47, 440–448, 1990.
- See, S. W., Wang, Y. H., and Balasubramanian, R.: Contrasting reactive oxygen species and transition metal concentrations in combustion aerosols, *Environ. Res.*, 103, 317–324, 2007.
- Spaulding, R. S., Talbot, R. W., and Charles, M. J.: Optimization of a Mist Chamber (Cofer Scrubber) for Sampling Water-Soluble Organics in Air, *Environ. Sci. Technol.*, 36, 1798–1808, 2002.
- Squadrito, G. L., Cueto, R., Dellinger, B., and Pryor, W. A.: Quinoid Redox Cycling as a Mechanism for Sustained Free Radical Generation by Inhaled Airborne Particulate Matter, *Free Radical Biol. Med.*, 31, 1132–1138, 2001.
- Stobbe, E. R., de Boer, B. A., and Geus, J. W.: The reduction and oxidation behaviour of manganese dioxides, *Catal. Today*, 47, 161–167, 1999.
- Sugamura, K. and Keaney, J., and John F.: Reactive oxygen species in cardiovascular disease, *Free Radical Biol. Med.*, 51, 978–992, 2011.
- Venkatachari, P. and Hopke, P. K.: Development and Laboratory Testing of an Automated Monitor for the Measurement of Atmospheric Particle-Bound Reactive Oxygen Species (ROS), *Aerosol Sci. Technol.*, 42, 629–635, doi:10.1080/02786820802227345, 2008.
- Venkatachari, P., Hopke, P. K., Grover, B. D., and Eatough, D. J.: Measurement of Particle-Bound Reactive Oxygen Species in Rubidoux Aerosols, *J. Atmos. Chem.*, 50, 49–58, 2005.

- Venkatachari, P., Hopke, P. K., Brune, W. H., Ren, X., Leshner, R., Mao, J., and Mitchell, M.: Characterization of Wintertime Reactive Oxygen Species Concentrations in Flushing, New York, *Aerosol Sci. Technol.*, 41, 97–111, doi:10.1080/02786820601116004, 2007.
- Votyakova, T. V. and Reynolds, I. J.: Detection of hydrogen peroxide with Amplex Red: interference by NADH and reduced glutathione auto-oxidation, *Arch. Biochem. Biophys.*, 431, 138–144, doi:10.1016/j.abb.2004.07.025, 2004.
- Wang, Y., Arellanes, C., Curtis, D. B., and Paulson, S. E.: Probing the Source of Hydrogen Peroxide Associated with Coarse Mode Aerosol Particles in Southern California, *Environ. Sci. Technol.*, 44, 4070–4075, 2010.
- Wang, Y., Hopke, P. K., Sun, L., Chalupa, D. C., and Utell, M. J.: Laboratory and field testing of an automated atmospheric particle-bound reactive oxygen species sampling-analysis system, *J. Toxicol.*, 2011, 9 pp., doi:10.1155/2011/419476, 2011.
- Xia, T., Kovoichich, M., Brant, J., Hotze, M., Sempf, J., Oberley, T., Sioutas, C., Yeh, J. I., Wiesner, M. R., and Nel, A.: Comparison of the Abilities of Ambient and Manufactured Nanoparticles To Induce Cellular Toxicity According to an Oxidative Stress Paradigm, *Nano Letters*, 6, 1794–1807, 2006.
- Zhou, M., Diwu, Z., Panchuk-Voloshina, N., and Haugland, R. P.: A Stable Nonfluorescent Derivative of Resorufin for the Fluorometric Determination of Trace Hydrogen Peroxide: Applications in Detecting the Activity of Phagocyte NADPH Oxidase and Other Oxidases, *Anal. Biochem.*, 253, 162–168, 1997.